

## DYNAMICS OF A CONTROLLED DISCRETE PREY-PREDATOR MODEL WITH HOLLING TYPE-II FUNCTIONAL RESPONSE

YANLIN MIN, XIAOLING HAN, AND CEYU LEI

**ABSTRACT.** This article investigates the complex dynamic behavior of a discrete predator-prey model with Holling type II functional response. Firstly, we discuss the local stability of the system at the equilibrium points. Secondly, we apply the central manifold theorem and bifurcation theory to demonstrate the existence of two different types of bifurcations within the system, namely flip and Hopf bifurcations. Through numerical simulation, we validate the impact of human control parameters of predators and the degree of predator utilization on system dynamics. The results indicate that studying the predator-prey relationships in plateau pastoral areas can assist in more accurately predicting changes in prey and predator populations, which is of great significance for ecosystem protection.

### 1. INTRODUCTION

In nature, no species exists in isolation, and it always has various connections with other species. The interaction between species is crucial for the survival and development of the entire biological community. It not only affects the survival of each species, but also connects them to a complex life network, determining the stability of communities and ecosystems. Predator-prey interaction is one of the basic relationships between biological populations, and is a hot topic in ecology and biomathematics. Predation is a common phenomenon where predators obtain nutrients by capturing prey, thereby maintaining their own lives. Therefore, studying predatory models is particularly important. By studying the stability of predatory population models, the development trend of populations can be explained and predicted, which has important guiding significance for protecting diversity of biological populations and maintaining sustainable development of ecosystems[3, 16, 10].

One application of nonlinear differential equations in mathematical biology is to model the predator-prey relationship of a simple ecosystem. Lotka(1925) and Volterra(1926) proposed the Lotka-Volterra(L-V)model to describe the interaction between two species. In this model, when the prey is lacking, the predator will become extinct. However, in the ecological environment, when the prey is scarce, the predator will look for other food resources. Therefore, in order to implement realistic assumptions in prey-predator model, more and more scholars have made different modifications on the basis of the L-V model[2, 13, 14]. Combined with the Holling type-II functional response function[8], Aziz-Alaoui and Daher Okiye [1] studied the following modified system :

$$\begin{cases} \frac{dx_1}{dt} = rx_1 \left(1 - \frac{x_1}{K}\right) - \frac{a_1 x_1 x_2}{n_1 + x_1}, \\ \frac{dx_2}{dt} = sx_2 \left(1 - \frac{a_2 x_2}{n_2 + x_1}\right), \end{cases} \quad (1.1)$$

---

Received by the editors 7 May 2024; accepted 30 August 2024; published online 21 September 2024.

2020 *Mathematics Subject Classification.* 92D25.

*Key words and phrases.* Discrete model; flip bifurcation; Hopf bifurcation; bifurcation theory; chaos.

X.-L. Han was supported in part by NSFC Grant 12161079.

where,  $x_1(t)$  and  $x_2(t)$  represent the population density of prey and predator,  $r$  and  $s$  represent the intrinsic growth rate of prey and predator,  $K$  represents the environmental carrying capacity,  $a_1$  is the maximum per capita prey reduction rate,  $a_2$  is the maximum value of the per capita reduction rate of predator,  $n_1$  and  $n_2$  measure the degree to which the environment provides protection for prey and predator, respectively. Aziz Alaoui and Daher Okiye [1] studied the boundedness of the solution of the model and the global stability of the positive equilibrium. Song and Li [18] studied a predator-prey system with pulse effects based on the Leslie-Gower scheme and Holling type-II scheme. By using Floquet theory of linear periodic impulsive equation, some conditions for the linear stability of trivial periodic solution and semi-trivial periodic solutions are obtained. On the basis of model (1.1), Zhu and Wang [20] use the coincidence theory and the Lyapunov function to prove the existence and global attraction of the positive periodic solution. In recent years, due to the unreasonable development of the ecosystem in pastoral areas, the ecological environment has been deteriorating continuously. In order to protect fragile pastoral ecosystems and promote harmonious coexistence between humans and nature, some scholars have established a series of predatory models to guide herders in rational grazing. In some regions, generations [11] of livestock will implement intermittent grazing to fully utilize resources and protect the ecological balance of grasslands. When facing predators, prey is not powerless and can also reduce their burden through methods such as toxicity [19] and attracting third-party obstacles [15]. Similarly, human control over the number of predators also has a certain impact on the ecological balance of the population. Based on the above viewpoint, in order to better maintain ecosystem balance, we establish a predator-prey model with human control:

$$\begin{cases} \frac{dN}{dt} = r_1 N(t) \left(1 - \frac{N(t)}{K}\right) - \frac{\beta_1 N(t)P(t)}{N(t) + a}, \\ \frac{dP}{dt} = r_2 P(t) \left(1 - \frac{P(t)}{hN(t) + c}\right) - \frac{\beta_2 N(t)P(t)}{N(t) + a} + kP(t), \end{cases} \quad (1.2)$$

where  $N(t)$  and  $P(t)$  represent the density of prey and predator at time  $t$ , respectively.  $\frac{\beta_1 P(t)}{N(t)+a}$  is the Holling type II functional response function, which represents the number of prey taken by a unit predator in a unit time and  $a$  is half of the saturated level,  $k$  represents artificial control of the number of predators. Many scholars have studied the population dynamics behavior of continuous time models, while discrete time models are suitable for non overlapping generations, such as annual plants or insect populations with only one generation per year, and are suitable for describing nonlinear dynamics and chaotic behavior [6, 4, 9, 5, 7, 17, 12]. And in the process of numerical simulation of continuous model, it is also necessary to discretize the continuous model. By using the forward Euler difference method, the model (1.2) can be written as:

$$\begin{cases} N(t+1) = N(t) + N(t) \left[ r_1 \left(1 - \frac{N(t)}{K}\right) - \frac{\beta_1 P(t)}{N(t) + a} \right], \\ P(t+1) = P(t) + P(t) \left[ r_2 \left(1 - \frac{P(t)}{hN(t) + c}\right) - \frac{\beta_2 N(t)}{N(t) + a} + k \right]. \end{cases} \quad (1.3)$$

To our knowledge, so far no one has analyzed the dynamic behavior of discrete model (1.3). This article will investigate the existence and bifurcation phenomena of the equilibrium points of model (1.3). This paper is organized as follows. In section 2, we give the existence and stability conditions of fixed points of model (1.3). In section 3, flip bifurcation and Hopf bifurcation are performed on discrete model. In section 4, we provide numerical simulations that not only illustrate the results of theoretical analysis, but also demonstrate complex and new dynamic behaviors. Finally, a summary and discussion are conducted on this article.

2. THE EXISTENCE AND STABILITY OF FIXED POINTS

The fixed points of model (1.3) satisfy the following equations:

$$\begin{cases} N = N + N \left[ r_1 \left( 1 - \frac{N}{K} \right) - \frac{\beta_1 P}{N + a} \right], \\ P = P + P \left[ r_2 \left( 1 - \frac{P}{hN + c} \right) - \frac{\beta_2 N}{N + a} + k \right]. \end{cases} \tag{2.1}$$

By simple calculation, we can obtain three non-negative fixed points:

$$\begin{aligned} E_0(N_0, P_0) &: (0, 0); \\ E_1(N_1, P_1) &: (K, 0); \\ E^*(N^*, P^*) &: \left( N^*, \frac{r_1 - (1 - N^*/K)(N^* + a)}{\beta_1} \right), \end{aligned}$$

where  $r_1 > (1 - \frac{N^*}{K})(N^* + a)$  and  $N^*$  is the positive root of following univariate cubic equations:

$$-r_2 N^3 + \mathfrak{A} N^2 + \mathfrak{B} N + \mathfrak{C} = 0,$$

where

$$\begin{aligned} \mathfrak{A} &= (K - 2a - hk\beta_1)r_2, \\ \mathfrak{B} &= ar_2(2k - a) + K\beta_1(K + \beta_2 - har_2K - cK), \\ \mathfrak{C} &= aK(c\beta_1r_2 + r_2a + K\beta_1). \end{aligned}$$

The Jacobian matrix corresponding to model (1.3) at the equilibrium point  $(N, P)$  is written as

$$J(N, P) = \begin{pmatrix} 1 + r_1 - \frac{2Nr_1}{K} - \frac{\beta_1 Pa}{(N+a)^2} & -\frac{N\beta_1}{N+a} \\ \frac{hP^2}{(hN+c)^2} - \frac{\beta_2 aP}{(N+a)^2} & 1 + r_2 - \frac{2Pr_2}{hN+c} - \frac{\beta_2 N}{N+a} + k \end{pmatrix}.$$

The characteristic equation of the Jacobian matrix can be written as

$$\lambda^2 - P(N, P)\lambda + Q(N, P) = 0,$$

where

$$P(N, P) = \text{tr}J, \quad Q(N, P) = \det J.$$

In order to study the modulus of eigenvalues of Jacobian matrix at the equilibrium point  $(N, P)$ , we give the following lemma.

**Lemma 2.1.** [7] *Assume that  $F(\lambda) = \lambda^2 - A\lambda + B$ , and  $F(1) > 0$  with  $\lambda_1, \lambda_2$  are roots of  $F(\lambda) = 0$ . Then the following results hold true:*

- (A<sub>11</sub>)  $|\lambda_1| < 1$  and  $|\lambda_2| < 1$  if and only if  $F(-1) > 0$  and  $B < 1$ ;
- (A<sub>22</sub>)  $|\lambda_1| > 1$  and  $|\lambda_2| > 1$  if and only if  $F(-1) > 0$  and  $B > 1$ ;
- (A<sub>33</sub>)  $|\lambda_1| < 1$  and  $|\lambda_2| > 1$ ,  $|\lambda_1| > 1$  and  $|\lambda_2| < 1$  if and only if  $F(-1) < 0$ ;
- (A<sub>44</sub>)  $\lambda_1 = -1$  and  $\lambda_2 \neq 1$  if and only if  $F(-1) = 0$  and  $B \neq 0, 2$ ;
- (A<sub>55</sub>)  $\lambda_1$  and  $\lambda_2$  are complex and  $|\lambda_1| = 1$  and  $|\lambda_2| = 1$  if and only if  $A^2 - 4B < 0$  and  $B = 1$ .

Suppose that  $\lambda_1$  and  $\lambda_2$  are the eigenvalues of the variational matrix  $J(N, P)$  evaluated at equilibrium point of model (1.3), The equilibrium point  $(N, P)$  is called a sink if  $|\lambda_1| < 1$  and  $|\lambda_2| < 1$ , the sink is locally asymptotically stable. The equilibrium point  $(N, P)$  is a source if  $|\lambda_1| > 1$  and  $|\lambda_2| > 1$ , the source is locally unstable. If either  $|\lambda_1| = 1$  or  $|\lambda_2| = 1$ , then the equilibrium point  $(N, P)$  is

non-hyperbolic. The equilibrium point  $(N, P)$  is a saddle if  $|\lambda_1| < 1$  and  $|\lambda_2| > 1$  ( or  $|\lambda_1| > 1$  and  $|\lambda_2| < 1$ ). By simple calculation, the Jacobian matrix for the discrete model (1.3) at  $E_0$  and  $E_1$

$$J(E_0) = \begin{pmatrix} 1+r_1 & 0 \\ 0 & 1+r_2+k \end{pmatrix}, J(E_1) = \begin{pmatrix} 1-r_1 & -\frac{K\beta_1}{K+a} \\ 0 & 1+r_2-\frac{K\beta_2}{K+a}+k \end{pmatrix}.$$

Through the above Lemma2.1, we analyze the stability of three equilibrium points and obtain the following proposition.

**Proposition 2.2.** *The eigenvalues of  $J(0, 0)$  are  $\lambda_1 = 1 + r_1$ ,  $\lambda_2 = 1 + r_2 + k$ , then*

- ( $\mathcal{B}_1$ )  $E_0(0, 0)$  is a saddle point if and only if  $-2 < r_2 + k < 0$ .
- ( $\mathcal{B}_2$ )  $E_0(0, 0)$  is a source if one of the following conditions holds:
  - (a)  $k > 1 - r_2$ ;
  - (b)  $k < -1 - r_2$ .
- ( $\mathcal{B}_3$ )  $E_0(0, 0)$  is non-hyperbolic if  $r_2 = -k$  or  $r_2 = -k - 2$ .

*Proof.* Obviously,  $|\lambda_1| > 1$  always holds, we only need  $|\lambda_2| < 1$  so that the condition hold, that is,  $-2 < r_2 + k < 0$ . Similarly, it can be concluded that  $\mathcal{B}_2$  and  $\mathcal{B}_3$ . □

**Proposition 2.3.** *The eigenvalues of  $J(K, 0)$  are  $\lambda_1 = 1 - r_1$ ,  $\lambda_2 = 1 + r_2 - \frac{\beta_2 K}{K+a} + k$ , then*

- ( $\mathcal{C}_1$ )  $E_1(K, 0)$  is sink if and only if  $r_2(K + 1) < \beta_2 K - k(K + a) < (2 + r_2)(K + 1)$ .
- ( $\mathcal{C}_2$ )  $E_1(K, 0)$  is a source point if one of the following conditions holds:
  - (a)  $k + r_2 > \frac{\beta_2 K}{K+a}$  and  $r_1 > 2$ ;
  - (b)  $k + r_2 + 2 < \frac{\beta_2 K}{K+a}$  and  $r_1 > 2$ .
- ( $\mathcal{C}_3$ )  $E_1(K, 0)$  is a saddle point if one of the following conditions holds:
  - (a)  $k + r_2 < \frac{\beta_2 K}{K+a} < k + r_2 + 2$  and  $r_1 > 2$ ;
  - (b)  $k + r_2 > \frac{\beta_2 K}{K+a}$  and  $0 < r_1 < 2$ ;
  - (c)  $k + r_2 + 2 < \frac{\beta_2 K}{K+a}$  and  $0 < r_1 < 2$ .
- ( $\mathcal{C}_4$ )  $E_0(K, 0)$  is non-hyperbolic if  $K(k + \beta_2 + r_2) = -r_2 - k$  or  $K(k + \beta_2 + r_2 + 2) = -r_2 - k - 2$ .

*Proof.* Obviously,  $|\lambda_1| < 1$  always holds, we only need  $|\lambda_2| < 1$  so that the condition hold, that is  $r_2(K + a) < \beta_2 K - k(K + a) < (2 + r_2)(K + a)$ . Similarly, it can be concluded that  $\mathcal{C}_2$ ,  $\mathcal{C}_3$  and  $\mathcal{C}_4$ . □

The Jacobian matrix computed at  $E^*(N^*, P^*)$  is

$$J(E^*) = \begin{pmatrix} 1+r_1-\frac{2N^*r_1}{K}-\frac{\beta_1P^*a}{(N^*+a)^2} & -\frac{N^*\beta_1}{N^*+a} \\ \frac{hP^{*2}}{(hN^*+c)^2}-\frac{\beta_2aP^*}{(N^*+a)^2} & 1+r_2-\frac{2P^*r_2}{hN^*+c}-\frac{\beta_2N^*}{N^*+a}+k \end{pmatrix}. \tag{2.2}$$

Therefore, the characteristic equation can be written as

$$\lambda^2 - (2 + G)\lambda + (1 + G + Q) = 0,$$

where

$$\begin{aligned} M(r_1) &= r_1 - \frac{2N^*r_1}{K} - \frac{\beta_1P^*a}{(N^*+a)^2}, \\ N(r_1) &= r_2 - \frac{2P^*r_2}{hN^*+c} - \frac{\beta_2N^*}{N^*+a} + k, \\ D(r_1) &= \frac{N^*\beta_1}{N^*+a} \left[ \frac{hP^{*2}}{(hN^*+c)^2} - \frac{\beta_2aP^*}{(N^*+a)^2} \right], \\ Q(r_1) &= M(r_1)N(r_1) + D(r_1), \quad G(r_1) = M(r_1) + N(r_1). \end{aligned}$$

Let

$$F(\lambda) = \lambda^2 - (2 + G)\lambda + (1 + G + Q). \tag{2.3}$$

Then

$$F(1) = Q, F(-1) = 4 + 2G + Q, F(0) = 1 + G + Q.$$

Through the above analysis, we can obtain the following proposition.

**Proposition 2.4.** *If the interior equilibrium point  $E^*(N^*, P^*)$  exists, then we have.*

- ( $\mathcal{D}_1$ )  $E^*(N^*, P^*)$  is sink if and only if  $\max\{0, -4 - 2G\} < Q < -G$ ;
- ( $\mathcal{D}_2$ )  $E^*(N^*, P^*)$  is a source point if and only if  $Q > 0, G > -4$  and  $G + Q > 0$ ;
- ( $\mathcal{D}_3$ )  $E^*(N^*, P^*)$  is a saddle if and only if  $0 < Q < -2G - 4$ ;
- ( $\mathcal{D}_4$ )  $E^*(N^*, P^*)$  is non-hyperbolic if one of the following conditions holds:
  - (a)  $Q = -2G - 4$  and  $G \neq -2, -4$ ,
  - (b)  $-2\sqrt{Q} < G < 0$  and  $Q = -G$ .

### 3. BIFURCATION ANALYSIS

Based on the above analysis, we will select  $r_1$  as the bifurcation parameter to perform flip and Hopf bifurcations of model (1.3).

**3.1. Flip bifurcation.** First of all, we will directly discuss the flip bifurcation of model (1.3) at  $E^*(N^*, P^*)$ . If the ( $\mathcal{D}_4$ ) of Proposition 2.3 holds, then one of the eigenvalues of the equilibrium point  $E^*(N^*, P^*)$  is -1 and the magnitude of the other is not equal to 1. Let's consider

$$\Omega_{FB1} = \{(r_1, r_2, K, a, h, \beta_1, \beta_2, c, k) \in \mathbb{R}_+^9 : Q = -2G - 4 \text{ and } G \neq -2, -4\}.$$

The unique positive equilibrium point  $E^*(N^*, P^*)$  of model (1.3) undergoes flip bifurcation. Taking  $r_1$  as small bifurcation parameter and a perturbation of model (1.3) in a small neighborhood of  $\Omega_{FB1}$ . At this point, we can write the model (1.3) in the following form:

$$\begin{cases} N \rightarrow N + N \left[ (r_1 + r_1^*) \left( 1 - \frac{N}{K} \right) - \frac{\beta_1 P}{N + a} \right], \\ P \rightarrow P + P \left[ r_2 \left( 1 - \frac{P}{hN + c} \right) - \frac{\beta_2 N}{N + a} + k \right], \end{cases} \tag{3.1}$$

where  $|r_1^*| \ll 1$ , which is a small bifurcation parameter. Taking  $\mathfrak{X} = N - N^*, \mathfrak{Y} = P - P^*$ , then the model (1.3) is converted into the following form

$$\begin{cases} \mathfrak{X} \rightarrow \mathfrak{a}_{11}\mathfrak{X} + \mathfrak{a}_{12}\mathfrak{Y} + \mathfrak{a}_{13}\mathfrak{X}^2 + \mathfrak{a}_{14}\mathfrak{X}\mathfrak{Y} + \mathfrak{a}_{15}\mathfrak{Y}^2 + \mathfrak{a}_{16}\mathfrak{X}^3 + \mathfrak{a}_{17}\mathfrak{X}^2\mathfrak{Y} + \mathfrak{a}_{18}\mathfrak{X}\mathfrak{Y}^2 + \\ \mathfrak{c}_1\mathfrak{X}r_1^* + \mathfrak{c}_2\mathfrak{Y}r_1^* + \mathfrak{c}_3\mathfrak{X}^2r_1^* + \mathfrak{c}_4\mathfrak{Y}^2r_1^* + \mathfrak{c}_5\mathfrak{X}\mathfrak{Y}r_1^* + O((|\mathfrak{X}| + |\mathfrak{Y}| + |r_1^*|)^4), \\ \mathfrak{Y} \rightarrow \mathfrak{b}_{11}\mathfrak{X} + \mathfrak{b}_{12}\mathfrak{Y} + \mathfrak{b}_{13}\mathfrak{X}^2 + \mathfrak{b}_{14}\mathfrak{X}\mathfrak{Y} + \mathfrak{b}_{15}\mathfrak{Y}^2 + \mathfrak{b}_{16}\mathfrak{X}^3 + \mathfrak{b}_{17}\mathfrak{X}^2\mathfrak{Y} + \mathfrak{b}_{18}\mathfrak{X}\mathfrak{Y}^2 + \\ O((|\mathfrak{X}| + |\mathfrak{Y}| + |r_1^*|)^4), \end{cases} \tag{3.2}$$

where

$$\begin{aligned}
\mathbf{a}_{11} &= 1 + r_1 - \frac{2N^*r_1}{K} - \frac{\beta_1 P^* a}{(N^* + a)^2}, \quad \mathbf{a}_{12} = -\frac{N^* \beta_1}{N^* + a}, \quad \mathbf{a}_{13} = -\frac{r_1}{K} + \frac{\beta_1 P^* a}{(N^* + a)^3}, \\
\mathbf{a}_{14} &= -\frac{\beta_1 a}{(N^* + a)^2}, \quad \mathbf{a}_{15} = 0, \quad \mathbf{a}_{16} = \frac{\beta_1 P^* a}{(N^* + a)^4}, \quad \mathbf{a}_{17} = \frac{\beta_1 a}{(N^* + a)^3}, \quad \mathbf{a}_{18} = 0, \\
\mathbf{b}_{11} &= \frac{hP^{*2}}{(hN^* + c)^2} - \frac{\beta_2 a P^*}{(N^* + a)^2}, \quad \mathbf{b}_{12} = 1 + r_2 - \frac{2P^* r_2}{hN^* + c} - \frac{\beta_2 N^*}{N^* + a} + k, \\
\mathbf{b}_{13} &= -\frac{hP^{*2}}{(hN^* + c)^3} + \frac{\beta_2 a P^*}{(N^* + a)^3}, \quad \mathbf{b}_{14} = 2\frac{hP^*}{(hN^* + c)^2} - \frac{\beta_2 a}{(N^* + a)^2}, \\
\mathbf{b}_{15} &= -\frac{h^2 P^{*2}}{(hN^* + c)^3} - \frac{\beta_2 a P^*}{(N^* + a)^3}, \quad \mathbf{b}_{16} = -\frac{h^3 P^{*2}}{(hN^* + c)^4} - \frac{\beta_2 a P^*}{(N^* + a)^4}, \\
\mathbf{b}_{17} &= -4\frac{h^2 P^*}{(hN^* + c)^3} + 2\frac{\beta_2 a}{(N^* + a)^3}, \quad \mathbf{b}_{18} = 2\frac{h}{(hN^* + c)^2}, \\
\mathbf{c}_1 &= -\frac{2N^*}{K}, \quad \mathbf{c}_2 = 0, \quad \mathbf{c}_3 = -\frac{1}{K}, \quad \mathbf{c}_4 = 0, \quad \mathbf{c}_5 = 0.
\end{aligned}$$

We can construct an invertible matrix

$$T_2 = \begin{pmatrix} \mathbf{a}_{12} & \mathbf{a}_{12} \\ -1 - \mathbf{a}_{11} & \lambda_2 - \mathbf{a}_{11} \end{pmatrix}, \quad (3.3)$$

and use the translation  $(\mathfrak{X}, \mathfrak{Y})^T = T_2(\mathfrak{U}, \mathfrak{V})^T$ , then (3.2) can be changed into

$$\begin{pmatrix} \mathfrak{U} \\ \mathfrak{V} \end{pmatrix} \rightarrow \begin{pmatrix} -1 & 0 \\ 0 & \lambda_2 \end{pmatrix} \begin{pmatrix} \mathfrak{U} \\ \mathfrak{V} \end{pmatrix} + \begin{pmatrix} f(\mathfrak{U}, \mathfrak{V}, r_1^*) \\ g(\mathfrak{U}, \mathfrak{V}, r_1^*) \end{pmatrix}, \quad (3.4)$$

where

$$\begin{aligned}
f(\mathfrak{U}, \mathfrak{V}, r_1^*) &= \frac{\mathbf{a}_{13}(\lambda_2 - \mathbf{a}_{11}) - \mathbf{b}_{13}\mathbf{a}_{12}}{\mathbf{a}_{12}(1 + \lambda_2)} \mathfrak{X}^2 + \frac{\mathbf{a}_{14}(\lambda_2 - \mathbf{a}_{11}) - \mathbf{b}_{14}\mathbf{a}_{12}}{\mathbf{a}_{12}(1 + \lambda_2)} \mathfrak{X}\mathfrak{V} \\
&+ \frac{\mathbf{a}_{16}(\lambda_2 - \mathbf{a}_{11}) - \mathbf{b}_{16}\mathbf{a}_{12}}{\mathbf{a}_{12}(1 + \lambda_2)} \mathfrak{X}^3 + \frac{\mathbf{a}_{17}(\lambda_2 - \mathbf{a}_{11}) - \mathbf{b}_{17}\mathbf{a}_{12}}{\mathbf{a}_{12}(1 + \lambda_2)} \mathfrak{X}^2 \\
&+ \frac{\mathbf{c}_1(\lambda_2 - \mathbf{a}_{11})}{\mathbf{a}_{12}(1 + \lambda_2)} \mathfrak{X}r_1^* + \frac{\mathbf{c}_3(\lambda_2 - \mathbf{a}_{11})}{\mathbf{a}_{12}(1 + \lambda_2)} \mathfrak{X}\mathfrak{V}r_1^* + O((|\mathfrak{X}| + |\mathfrak{V}| + |r_1^*|)^4), \\
g(\mathfrak{U}, \mathfrak{V}, r_1^*) &= \frac{\mathbf{a}_{13}(1 + \mathbf{a}_{11}) + \mathbf{b}_{13}\mathbf{a}_{12}}{\mathbf{a}_{12}(1 + \lambda_2)} \mathfrak{X}^2 + \frac{\mathbf{a}_{14}(1 + \mathbf{a}_{11}) + \mathbf{b}_{14}\mathbf{a}_{12}}{\mathbf{a}_{12}\mathbf{a}_{12}(1 + \lambda_2)} \mathfrak{X}\mathfrak{V} + \frac{\mathbf{a}_{16}(1 + \mathbf{a}_{11}) + \mathbf{b}_{16}\mathbf{a}_{12}}{\mathbf{a}_{12}(1 + \lambda_2)} \mathfrak{X}^3 \\
&+ \frac{\mathbf{a}_{17}(1 + \mathbf{a}_{11}) + \mathbf{b}_{17}\mathbf{a}_{12}}{\mathbf{a}_{12}(1 + \lambda_2)} \mathfrak{X}^2\mathfrak{V} + \frac{\mathbf{c}_1(1 + \mathbf{a}_{11})}{\mathbf{a}_{12}(1 + \lambda_2)} \mathfrak{X}r_1^* + \frac{\mathbf{c}_3(1 + \mathbf{a}_{11})}{\mathbf{a}_{12}(1 + \lambda_2)} \mathfrak{X}\mathfrak{V}r_1^* \\
&+ O((|\mathfrak{X}| + |\mathfrak{V}| + |r_1^*|)^4), \\
\mathfrak{X} &= \mathbf{a}_{12}\mathfrak{U} + \mathbf{a}_{12}\mathfrak{V}, \quad \mathfrak{V} = -(1 + \mathbf{a}_{11})\mathfrak{U} + (\lambda_2 - \mathbf{a}_{11})\mathfrak{V}.
\end{aligned}$$

Applying the central manifold theorem at evaluated  $(0,0)$  of the small neighborhood  $r_1^*$ , then  $W^c(0, 0, 0)$  can be approximated as follows:

$$W^c(0, 0, 0) = \{(\mathfrak{U}, \mathfrak{V}, r_1^*) \in R^3 | \mathfrak{V} = n^*(\mathfrak{U}, r_1^*) = \mathbf{a}_1\mathfrak{U}^2 + \mathbf{a}_2\mathfrak{U}r_1^* + \mathbf{a}_3r_1^{*2} + O((|\mathfrak{U}| + |r_1^*|)^3)\}. \quad (3.5)$$

Then the central manifold must satisfy

$$\mathfrak{M}(n^*(\mathfrak{U}, r_1^*)) = n^*(-\mathfrak{U} + f(\mathfrak{U}, \mathfrak{V}, r_1^*) - \lambda_2\mathfrak{V} - g(\mathfrak{U}, \mathfrak{V}, r_1^*)) = 0. \quad (3.6)$$

Next, by substituting (3.4) and (3.5) into (3.6) and comparing their coefficients of (3.5), we can obtain

$$\mathbf{a}_1 = \frac{\mathbf{a}_{12}^2[\mathbf{a}_{13}(1 + \mathbf{a}_{11}) + \mathbf{a}_{12}\mathbf{b}_{13}] + [(1 + \mathbf{a}_{11})^2\mathbf{a}_{14} + \mathbf{b}_{14}\mathbf{a}_{12}]}{\mathbf{a}_{12}(1 - \lambda_2^2)}, \quad \mathbf{a}_2 = \frac{\mathbf{c}_1(1 + \mathbf{a}_{11})}{\mathbf{a}_{12}(1 + \lambda_2)^2}, \quad \mathbf{a}_3 = 0.$$

Hence, the model (1.3) restricted to the center manifold is given by

$$F : \mathfrak{U} \rightarrow -\mathfrak{U} + n_1\mathfrak{U}^2 + n_2\mathfrak{U}r_1^* + n_1\mathfrak{U}^2 + n_4\mathfrak{U}r_1^{*2} + n_5\mathfrak{U}^3 + O((|\mathfrak{U}| + |r_1^*|)^4),$$

where

$$\begin{aligned} n_1 &= \frac{\mathbf{a}_{12}\mathbf{a}_{13}(\lambda_2 - \mathbf{a}_{11}) - \mathbf{a}_{12}^2\mathbf{b}_{13}}{1 + \lambda_2} + \frac{(\mathbf{a}_{11} + 1)[(\lambda_2 - \mathbf{a}_{11})\mathbf{a}_{14} - \mathbf{a}_{12}\mathbf{b}_{14}]}{1 + \lambda_2}, \\ n_2 &= \frac{(\lambda_2 - \mathbf{a}_{11})\mathbf{c}_1}{1 + \lambda_2}, \\ n_3 &= \frac{[\mathbf{a}_{14}(\lambda_2 - \mathbf{a}_{11}) - \mathbf{a}_{12}\mathbf{b}_{14}][(\lambda_2 - \mathbf{a}_{11})\mathbf{a}_2]}{1 + \lambda_2} - \frac{(1 + \mathbf{a}_{11})\mathbf{a}_{12}\mathbf{a}_2[\mathbf{a}_{14}(\lambda_2 - \mathbf{a}_{11}) - \mathbf{a}_{12}\mathbf{b}_{14}]}{1 + \lambda_2} \\ &\quad + \frac{\mathbf{a}_{12}\mathbf{c}_3(\lambda_2 - \mathbf{a}_{11})}{1 + \lambda_2} + \frac{\mathbf{a}_1\mathbf{c}_1(\lambda_2 - \mathbf{a}_{11})}{1 + \lambda_2}, \\ n_4 &= \frac{\mathbf{a}_2\mathbf{c}_1(\lambda_2 - \mathbf{a}_{11})}{1 + \lambda_2}, \\ n_5 &= \frac{\mathbf{a}_{16}\mathbf{a}_{12}(\lambda_2 - \mathbf{a}_{11}) - \mathbf{a}_{12}^3\mathbf{b}_{16}}{1 + \lambda_2} + \frac{[\mathbf{a}_{14}(\lambda_2 - \mathbf{a}_{11}) - \mathbf{a}_{12}\mathbf{b}_{14}][(\lambda_2 - \mathbf{a}_{11})\mathbf{a}_1]}{1 + \lambda_2} \\ &\quad - \frac{[(1 + \mathbf{a}_{11})\mathbf{a}_{12}][(\lambda_2 - \mathbf{a}_{11})\mathbf{a}_{17} - \mathbf{a}_{12}\mathbf{b}_{17}]}{1 + \lambda_2}. \end{aligned}$$

Let

$$\gamma_1 = \left[ \frac{\partial^2 F}{\partial \mathfrak{U} \partial r_1^*} + \frac{1}{2} \frac{\partial F}{\partial r_1^*} \frac{\partial^2 F}{\partial \mathfrak{U}^2} \right]_{(0,0)} = n_2, \quad \gamma_2 = \left[ \frac{1}{6} \frac{\partial^3 F}{\partial \mathfrak{U}^3} + \left( \frac{1}{2} \frac{\partial^2 F}{\partial \mathfrak{U}^2} \right)^2 \right]_{(0,0)} = n_5 + n_1^2.$$

From the above analysis, we obtain the following theorem.

**Theorem 3.1.** *The interior equilibrium point  $(N^*, P^*)$  loses its stability via flip bifurcation if  $\gamma_1 \neq 0$  and  $\gamma_2 \neq 0$ . Moreover, if  $\gamma_2 > 0$ , then the periof-2 orbits bifurcating from  $(N^*, P^*)$  are stable, on the contrary, it is unstable.*

**3.2. Hopf bifurcation.** From the analysis above, We consider model (1.3) with arbitrary parameter  $(r_1, r_2, K, a, h, \beta_1, \beta_2, c, k) \in \Omega_{HF}$ , where

$$\Omega_{HF} = \{(r_1, r_2, K, a, h, \beta_1, \beta_2, c, k) \in \mathbb{R}_+^9 : 1 + N(r_1) < 0, -2\sqrt{G} < Q < 0 \text{ and } Q = -G\},$$

which is described as below:

$$\begin{cases} N \rightarrow N + N \left[ (r_1 + r_1^*) \left( 1 - \frac{N}{K} \right) - \frac{\beta_1 P}{N + a} \right], \\ P \rightarrow P + P \left[ r_2 \left( 1 - \frac{P}{hN + c} \right) - \frac{\beta_2 N}{N + a} + k \right]. \end{cases} \quad (3.7)$$

Taking  $\mathfrak{X} = N - N^*$ ,  $\mathfrak{Y} = P - P^*$ , then model (1.3) is converted into the following form:

$$\begin{cases} \mathfrak{X} \rightarrow \mathbf{a}_{11}\mathfrak{X} + \mathbf{a}_{12}\mathfrak{Y} + \mathbf{a}_{13}\mathfrak{X}^2 + \mathbf{a}_{14}\mathfrak{X}\mathfrak{Y} + \mathbf{a}_{15}\mathfrak{Y}^2 + \mathbf{a}_{16}\mathfrak{X}^3 + \mathbf{a}_{17}\mathfrak{X}^2\mathfrak{Y} + \mathbf{a}_{18}\mathfrak{X}\mathfrak{Y}^2 + O(|\mathfrak{X}| + |\mathfrak{Y}|^4), \\ \mathfrak{Y} \rightarrow \mathbf{b}_{11}\mathfrak{X} + \mathbf{b}_{12}\mathfrak{Y} + \mathbf{b}_{13}\mathfrak{X}^2 + \mathbf{b}_{14}\mathfrak{X}\mathfrak{Y} + \mathbf{b}_{15}\mathfrak{Y}^2 + \mathbf{b}_{16}\mathfrak{X}^3 + \mathbf{b}_{17}\mathfrak{X}^2\mathfrak{Y} + \mathbf{b}_{18}\mathfrak{X}\mathfrak{Y}^2 + O(|\mathfrak{X}| + |\mathfrak{Y}|^4), \end{cases} \quad (3.8)$$

where  $\mathbf{a}_{11}, \mathbf{a}_{12}, \mathbf{a}_{13}, \mathbf{a}_{14}, \mathbf{a}_{15}, \mathbf{a}_{16}, \mathbf{a}_{17}, \mathbf{a}_{18}, \mathbf{b}_{11}, \mathbf{b}_{12}, \mathbf{b}_{13}, \mathbf{b}_{14}, \mathbf{b}_{15}, \mathbf{b}_{16}, \mathbf{b}_{17}, \mathbf{b}_{18}$  are given in (3.4) by substituting  $r_1$  for  $r_1 + r_1^*$ . The characteristic equation of map (3.8) at  $(N^*, P^*)$  is given by

$$\lambda^2 + p(r_1^*)\lambda + q(r_1^*) = 0$$

where

$$p(r_1^*) = -2 - G(r_1 + r_1^*), q(r_1^*) = 1 + G(r_1 + r_1^*) + Q(r_1 + r_1^*).$$

It is not difficult to see that the eigenvalues of the above quadratic equation are a pair of complex conjugate numbers  $\lambda$  and  $\bar{\lambda}$  with modulus 1 by Proposition 2.3, where

$$\lambda, \bar{\lambda} = -\frac{p(r_1^*) \pm i\sqrt{4q(r_1^*) - p^2(r_1^*)}}{2}.$$

When  $r_1^*$  changes in limited neighborhood of  $r_1^* = 0$ , then we have

$$\lambda(0), \bar{\lambda}(0) = 1 + \frac{G}{2} \pm \frac{\sqrt{4Q - G^2}}{2}i = \alpha \pm \beta i,$$

so, we can get

$$|\lambda(r_1^*)| = \sqrt{q(r_1^*)}, d = \frac{d|\lambda(r_1^*)|}{d(r_1^*)} \Big|_{r_1^*=0} = -\frac{N^*}{2}(1 + N(r_1)) > 0.$$

Since  $(r_1, r_2, K, a, h, \beta_1, \beta_2, c, k) \in \Omega_{HF}$ , we get  $p(0) \neq 0, 1, 2, -2$ , and hence,  $\lambda^m(0), \bar{\lambda}^m(0) \neq 1$  for all  $m=1,2,3,4$  at  $r_1^* = 0$ . Next, we discuss the normal form corresponding to model (1.3) when  $r_1^* = 0$ . Using the following translation

$$\begin{pmatrix} \mathfrak{X} \\ \mathfrak{Y} \end{pmatrix} = \begin{pmatrix} \mathbf{a}_{12} & 0 \\ \alpha - \mathbf{a}_{11} & -\beta \end{pmatrix} \begin{pmatrix} \mathfrak{U} \\ \mathfrak{V} \end{pmatrix}, \tag{3.9}$$

that is  $\mathfrak{X} = \mathbf{a}_{12}\mathfrak{U}, \mathfrak{Y} = (\alpha - \mathbf{a}_{11})\mathfrak{U} - \beta\mathfrak{V}$ . Let  $\alpha = -p(0)/2, \beta = \sqrt{4q(0) - p^2(0)}/2$ , then (3.8) becomes

$$\begin{pmatrix} \mathfrak{U} \\ \mathfrak{V} \end{pmatrix} \rightarrow \begin{pmatrix} \alpha & -\beta \\ \beta & \alpha \end{pmatrix} \begin{pmatrix} \mathfrak{U} \\ \mathfrak{V} \end{pmatrix} + \begin{pmatrix} \bar{f}(\mathfrak{U}, \mathfrak{V}) \\ \bar{g}(\mathfrak{U}, \mathfrak{V}) \end{pmatrix}, \tag{3.10}$$

where

$$\begin{aligned} \bar{f} &= \frac{\mathbf{a}_{13}}{\mathbf{a}_{11}}\mathfrak{X}^2 + \frac{\mathbf{a}_{14}}{\mathbf{a}_{11}}\mathfrak{X}\mathfrak{Y}^2 + \frac{\mathbf{a}_{16}}{\mathbf{a}_{11}}\mathfrak{X}^3 + \frac{\mathbf{a}_{17}}{\mathbf{a}_{11}}\mathfrak{X}^2\mathfrak{Y} + O((|\mathfrak{X}| + |\mathfrak{Y}|)^4), \\ \bar{g} &= \frac{\mathbf{a}_{13}(\alpha - \mathbf{a}_{11}) - \mathbf{b}_{13}\mathbf{a}_{12}}{\mathbf{a}_{11}\beta}\mathfrak{X}^2 + \frac{\mathbf{a}_{14}(\alpha - \mathbf{a}_{11}) - \mathbf{b}_{14}\mathbf{a}_{12}}{\mathbf{a}_{11}\beta}\mathfrak{X}\mathfrak{Y} + \frac{\mathbf{a}_{16}(\alpha - \mathbf{a}_{11}) - \mathbf{b}_{16}\mathbf{a}_{12}}{\mathbf{a}_{11}\beta}\mathfrak{X}^3 \\ &\quad + \frac{\mathbf{a}_{17}(\alpha - \mathbf{a}_{11}) - \mathbf{b}_{17}\mathbf{a}_{12}}{\mathbf{a}_{11}\beta}\mathfrak{X}^2\mathfrak{Y} + O((|\mathfrak{X}| + |\mathfrak{Y}|)^4). \end{aligned}$$

Next, We define the following nonzero real number:

$$L = - \left[ \text{Re} \left( \frac{(1 - 2\lambda)\bar{\lambda}^2}{1 - \lambda} \xi_{11}\xi_{12} \right) - \frac{1}{2}|\xi_{11}|^2 - |\xi_{02}|^2 + \text{Re}(\bar{\lambda}\xi_{21}) \right]_{r_1^*=0},$$

where

$$\begin{aligned} \xi_{20} &= \frac{1}{8}[(\bar{f}_{\mathfrak{U}\mathfrak{U}} - \bar{f}_{\mathfrak{V}\mathfrak{V}} + 2\bar{g}_{\mathfrak{U}\mathfrak{V}}) + i(\bar{g}_{\mathfrak{U}\mathfrak{U}} - \bar{g}_{\mathfrak{V}\mathfrak{V}} - 2\bar{f}_{\mathfrak{U}\mathfrak{V}})], \\ \xi_{11} &= \frac{1}{4}[(\bar{f}_{\mathfrak{U}\mathfrak{U}} + \bar{f}_{\mathfrak{V}\mathfrak{V}}) + i(\bar{g}_{\mathfrak{U}\mathfrak{U}} + \bar{g}_{\mathfrak{V}\mathfrak{V}})], \\ \xi_{02} &= \frac{1}{8}[(\bar{f}_{\mathfrak{U}\mathfrak{U}} - \bar{f}_{\mathfrak{V}\mathfrak{V}} - 2\bar{g}_{\mathfrak{U}\mathfrak{V}}) + i(\bar{g}_{\mathfrak{U}\mathfrak{U}} - \bar{g}_{\mathfrak{V}\mathfrak{V}} + 2\bar{f}_{\mathfrak{U}\mathfrak{V}})], \\ \xi_{21} &= \frac{1}{16}[(\bar{f}_{\mathfrak{U}\mathfrak{U}\mathfrak{U}} + \bar{f}_{\mathfrak{U}\mathfrak{V}\mathfrak{V}} + \bar{g}_{\mathfrak{U}\mathfrak{U}\mathfrak{V}} + \bar{g}_{\mathfrak{V}\mathfrak{V}\mathfrak{V}}) + i(\bar{g}_{\mathfrak{U}\mathfrak{U}\mathfrak{U}} + \bar{g}_{\mathfrak{U}\mathfrak{V}\mathfrak{V}} - \bar{g}_{\mathfrak{U}\mathfrak{U}\mathfrak{V}} - \bar{g}_{\mathfrak{V}\mathfrak{V}\mathfrak{V}})]. \end{aligned}$$

Through the above analysis, we have obtained the following result.

**Theorem 3.2.** *If  $L \neq 0$ , then model (1.3) passes through a Hopf bifurcation at the equilibrium point  $E^*(N^*, P^*)$  when the parameter  $r_1^*$  alters in the small region of the point  $(0, 0)$ . Also, if  $L > 0$  (resp.,  $L < 0$ ), then an repelling (resp., attracting) invariant closed curve bifurcates from equilibrium point  $E^*(N^*, P^*)$  for  $r_1^* > 0$  (resp.,  $r_1^* > 0$ ). It also implies that the both species in the system coexist under some specific conditions.*

#### 4. NUMERICAL SIMULATIONS

In this section, we use MATLAB to draw the bifurcation diagrams, phase portraits, and maximum Lyapunov exponents of model (1.3) to verify the theoretical analysis above and demonstrate complex and interesting dynamic behaviors.

##### (i) Flip bifurcation

Firstly, in Fig 1, we select the value of the bifurcation parameter  $r_1$  to vary in the range  $2 < r_1 < 3$ , while the other parameter values are fixed as  $r_2 = 0.8$ ,  $K = 5$ ,  $a = 0.1$ ,  $h = 0.5$ ,  $\beta_1 = 0.8$ ,  $\beta_2 = 0.5$  and  $c = 0.6$  with the initial value of  $(N_0, P_0) = (1, 1)$  and choose  $k = 0$ , that is unmanned control. Through Theorem 3.1, we can get the bifurcation critical value  $r_1 = 2.407$ , then model (1.3) undergoes flip bifurcation at equilibrium point  $(1.12355, 4.57496)$ . It is stable when  $r_1 < 2.407$ , and when  $r_1 > 2.407$ , model (1.3) oscillates with periods of 2, 4, 8, and so on. It can be obtained from Fig 1 (c) that as the bifurcation parameter  $r_1$  continues to increase, chaos may occur in model (1.3). Fig 1 (a), (b) are the bifurcation diagram of  $N$  and  $P$  with parameter  $r_1$ , (c) is the maximum Lyapunov exponent (MLE) diagram corresponding to Fig 1 (a) and Fig 1 (b). Similarly, the positive Lyapunov exponent in (c) indicates the occurrence of chaos.

In Fig 2, we show the phase portraits corresponding to the 2, 4, 8 periodic orbits when the parameters change and the irregular chaotic attractor when  $r_1 > 2.407$ . Obviously, in Fig 2 (a), (b), and (c) respectively represent the appearance of the period 2, period 4, and period 8 orbits of model (1.3) when  $r_1$  is taken as 2.62, 2.78, and 2.88. In Fig 2 (d), it shows the appearance of chaotic orbits. Similarly, we provide images of different solutions corresponding to different bifurcation parameters in Fig 2. The (e)-(h) in fig 2 correspond to (a)-(d), which is the image of the periodic solution obtained when selecting different parameters. In addition, as  $r_1$  continues to increase, the value of the maximum Lyapunov exponent related to model (1.3) is greater than 0, resulting in chaos, i.e. where the solution of the model (1.3) is arbitrarily periodic. Next, we fix the initial value and select separately  $k=0.3$ ,  $k=0.15$ ,

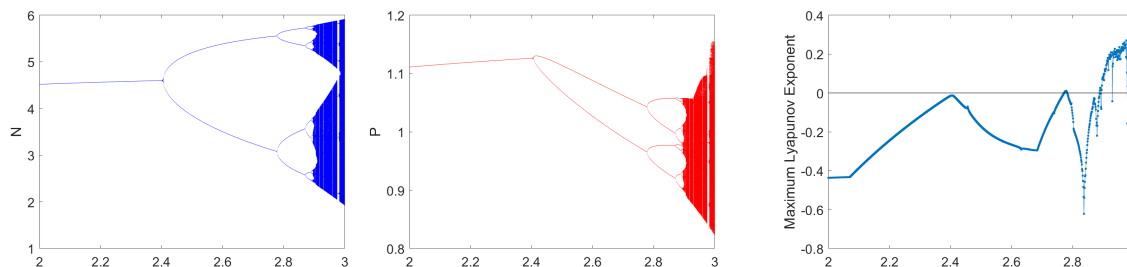


FIGURE 1. (a) Bifurcation diagram of system (3) with  $r_1 \in [2, 3]$ ,  $r_2 = 0.8$ ,  $K = 5$ ,  $a = 0.1$ ,  $h = 0.5$ ,  $\beta_1 = 0.8$ ,  $\beta_2 = 0.5$ ,  $c = 0.6$  and  $k = 0$ , the initial value is  $(N_0, P_0) = (1, 1)$ . (c) Maximum Lyapunov exponents corresponding to (a).

$k = -0.15$  and  $k = -0.3$  and keep other parameters of model (1.3) unchanged. From the bifurcation diagram, it can be clearly seen that human control parameter has a significant impact on the dynamic behavior of the population when the other bifurcation parameters remain unchanged. We can clearly observe in Fig

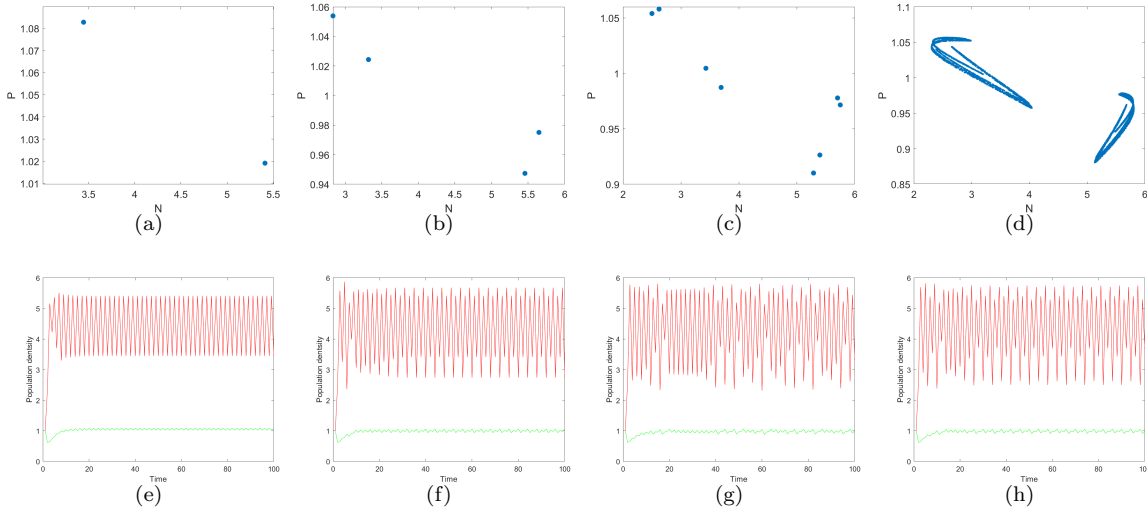


FIGURE 2. Phase portraits corresponding to Fig 1, which are obtained by ignoring 5000 discrete time unit transients and iterating 10000 times. (a) Period 2 orbits for  $r_1 = 2.62$ ; (b) Period 4 orbits for  $r_1 = 2.78$ ; (c) Period 8 orbits for  $r_1 = 2.88$ ; (d) A chaotic attractor for  $r_1 = 2.93$ .

3 that as  $k$  gradually decreases, model (1.3) undergoes chaotic phenomena from the periodic solution. When  $k=0.3$ , a period 2 orbit appears, and when  $k=0.15$ , a period 4 orbit appears; When  $k=-0.15$  and  $-0.3$ , chaos occurs as  $r_1$  increases, and as  $k$  gradually decreases, the bifurcation point of model (1.3) also shifts to lower values. This indicates that artificially increasing the number of predators will stabilize the system and prevent chaos. We also present the maximum Lyapunov exponent plots corresponding to different  $k$  in Fig 3. (ii) Hopf bifurcation Now, varying  $r_1$  in the range  $2.8 < r_1 < 3.4$  and fixing

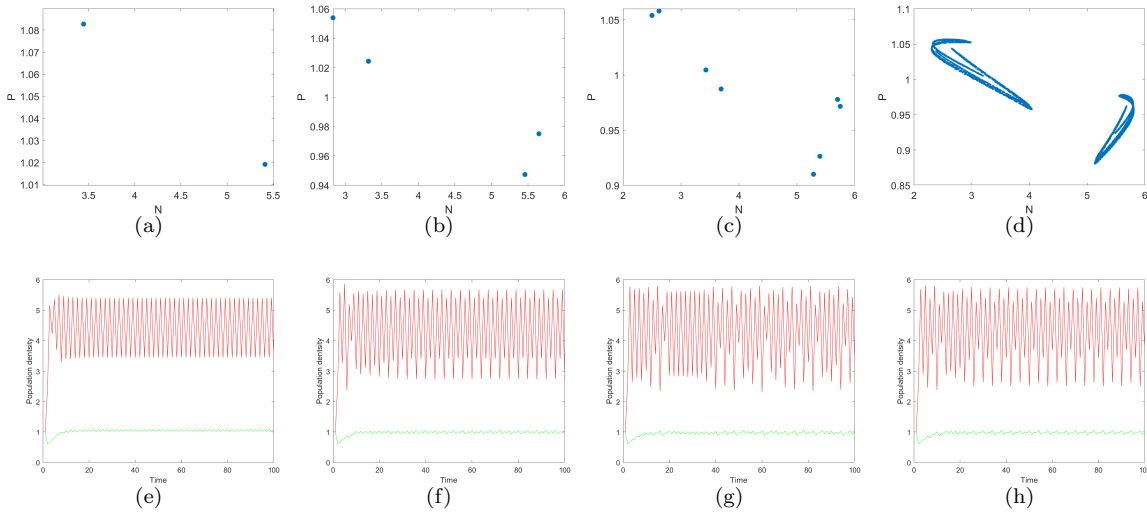


FIGURE 3. Phase portraits corresponding to Fig 1, which are obtained by ignoring 5000 discrete time unit transients and iterating 10000 times. (a) Period 2 orbits for  $r_1 = 2.62$ ; (b) Period 4 orbits for  $r_1 = 2.78$ ; (c) Period 8 orbits for  $r_1 = 2.88$ ; (d) A chaotic attractor for  $r_1 = 2.93$ .

$r_2 = 0.8, K = 5, a = 0.1, h = 4.7, \beta_1 = 0.8, \beta_2 = 0.5, c = 0.6, k = 0$ , the initial value is  $(N_0, P_0) = (1, 1)$ . By calculation, we know Hopf bifurcation emerges only from  $E^*(N^*, P^*) = (2.62832, 5.10335)$  at  $r_1 = 3.1442$ . That is to say, when  $r_1 = 3.1442$ , model(3) loses stability at the unique positive equilibrium

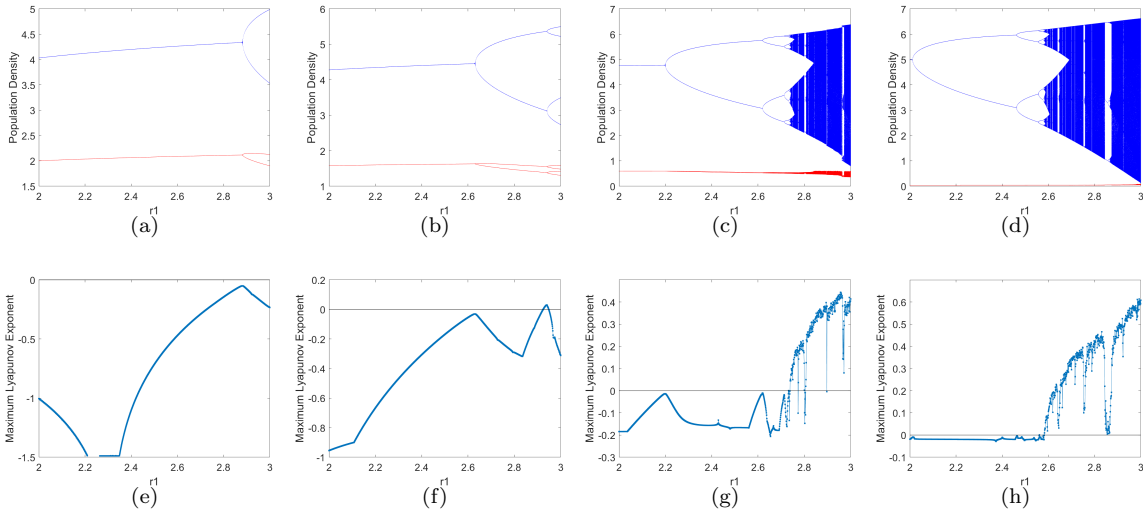


FIGURE 4. (a) and (d) Bifurcation diagram of model (2) when  $k = 0.3, 0.15, -0.15, -0.3$ , (e) to (h) maximum Lyapunov exponents corresponding to (a) to (d), the blue and red curves respectively represent  $N$  and  $P$ .

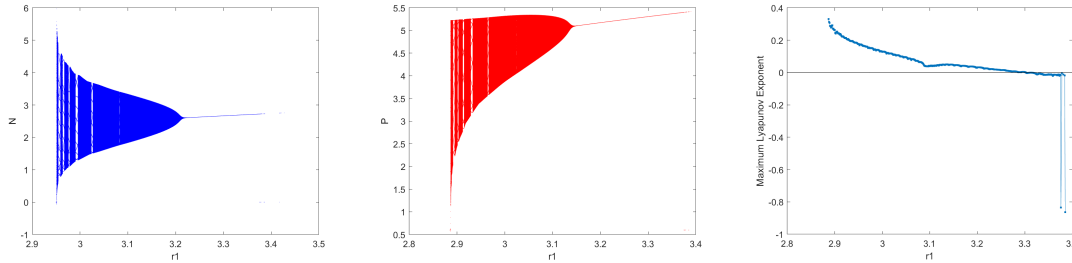


FIGURE 5. (a) Bifurcation diagram of system (4) with  $r_1 \in [2.8, 3.4]$ ,  $r_2 = 0.8, K = 5, a = 0.1, h = 4.7, \beta_1 = 0.8, \beta_2 = 0.5, c = 0.6, k = 0$ , the initial value is  $(N, P) = (1, 1)$ . (c) Maximum Lyapunov exponents corresponding to (a).

point  $E^*$  and generates closed invariant curve appears. In Fig 4, the bifurcation diagrams for  $N$  and  $P$  are shown in Fig 4(a) and (b), respectively. Moreover, the MLE are plotted in Fig 4(c). Furthermore, when  $h = 4.7$  and other parameters remain unchanged, compare with Fig 1, the bifurcation at the positive equilibrium point changes from flip bifurcation to Hopf bifurcation. So it can be concluded that the capture effect has a significant effect on the dynamic behaviour of model (1.3). From Fig 4 (a), we see that the equilibrium point is stable for  $r_1 > 3.1442$ , loses its stability at  $r_1 = 3.1442$  and a stable invariant cycle bifurcates from the equilibrium point  $(2.62832, 5.10335)$  for  $r_1 > 3.1442$ , some period orbits emerge in the period-windows. For example, an invariant cycle for  $r_1 = 3.122$ ; period-14 orbits for  $r_1 = 2.9152$ ; the orbits approach to chaos with the decreasing of  $r_1 = 2.888$ . Fig 5 (a) and (c) display how a smooth invariant circle bifurcates from the equilibrium point when  $r_1 < 3.1442$ , then the stable circle disappears and period-14 orbits and chaotic orbits appear.

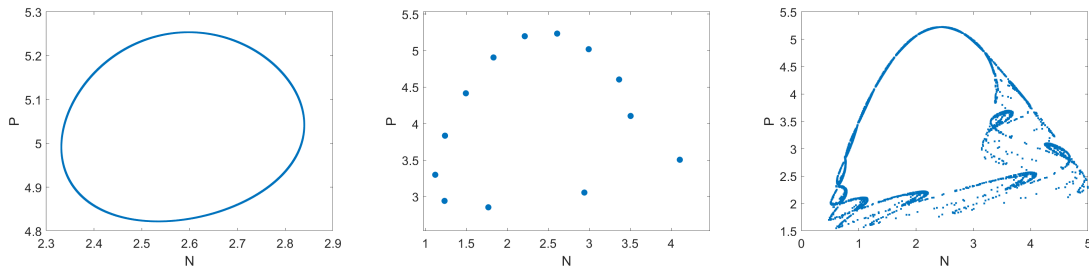


FIGURE 6. Phase portraits corresponding to Fig 4, an invariant cycle for  $r_1 = 3.122$  ;  
(b)period-14 orbits for  $r_1 = 2.9152$  ; (c) Chaotic orbits for  $r_1 = 2.888$ .

## 5. CONCLUSION

This article mainly studies the stability of the equilibrium of a discrete-time predator-prey model, as well as flip bifurcation and Hopf bifurcation. The rich dynamic behavior of model (1.3) is verified through bifurcation diagrams, maximum Lyapunov exponent diagrams, and phase diagrams. The research results indicate that the model (1.3) has three equilibrium points, and when condition  $(\mathcal{D}_1)$  holds, the positive equilibrium point  $E^*$  is locally asymptotically stable, where the predator and prey coexist. When the model parameters meet certain parameters, model (1.3) undergoes flip bifurcation and Hopf bifurcation at the positive equilibrium point. Numerical simulation results indicate that as the predator's utilization of prey increases, the model (1.3) undergoes a transition from flip bifurcation to Hopf bifurcation. However, when the control parameter  $k$  is gradually increased, the system does not exhibit chaotic phenomena. Therefore, the results of this study have important value for population control strategies in the ecosystem of plateau pastoral areas.

## REFERENCES

- [1] M. A. Aziz-Alaoui and M. Daher Okiye, *Boundedness and global stability for a predator-prey model with modified Leslie-Gower and Holling-type II schemes*, Appl. Math. Lett. **16**(2003) 1069-1075.
- [2] D. Y. Bai and X. X. Zhang, *Dynamics of a predator prey model with the additive predation in prey*, Mathematics, **10**(2022), 655.
- [3] A. A. Berryman, *The origins and evolution of predator-prey theory*, Ecology **73**(1992), 1530-1535.
- [4] Q. Din, *Complexity and chaos control in a discrete-time prey-predator model*, Commun. Nonlinear Sci. Numer. Simulat. **49**(2017), 113-134.
- [5] E. Elabbasy, A. Elsadany and Y. Zhang, *Bifurcation analysis and chaos in a discrete reduced Lorenz system*, Appl. Math. Comput. **228**(2014), 184-194.
- [6] S. Elaydi, *An Introduction to Difference Equations*, Springer, New York, 1996.
- [7] X. L. Han and C.Y. Lei, *Bifurcation and Turing instability analysis for a space- and time-discrete predator-prey system with Smith growth function*, Chaos, Solitons and Fractals **166**(2023): 112910.
- [8] C. S. Holling, *The Functional response of predators to prey density and its role in mimicry and population regulation*, Mem. Entomol. Soc. Can. **97**(1965), 5-60.
- [9] J. C. Huang, S. H. Liu, S. G. Ruan and D. M. Xiao, *Bifurcations in a discrete predator-prey model with non-monotonic functional response*, J. Math. Anal. Appl. **49**(2018), 201-230.
- [10] J. C. Huang, S. G. Ruan and J. Song, *Bifurcations in a predator-prey system of Leslie type with generalized Holling type III functional response*, J. Differ. Eqns. **257**(2014), 1721-1752.
- [11] W. L. Li, C. L. Liu, W. Y. Wang, H. K. Zhou, Y. T. Xue, J. Xu, P. F. Xue and H. P. Yan, *Effects of different grazing disturbances on the plant diversity and ecological functions of alpine grassland ecosystem on the Qinghai-Tibetan plateau*, Front. Plant Sci. **12**(2021), 765070.
- [12] C. Y. Lei, X. L. Han and W. M. Wang, *Bifurcation analysis and chaos control of a discrete-time prey-predator model with fear factor*, Math. Biosci. Eng. **19**(2022), 6659-6679.

- [13] X. C. Meng and M. S. Hari, *Stability of bifurcating solution of a predator prey model*, Chaos, Solitons and Fractals, **168**(2023), 113153.
- [14] Y. X. Meng, X. H. Meng and L. Zhong, *Dynamics of a modified Leslie-Gower predator-prey model with double Allee effects*, Math. Bios. Eng. **21**(2024), 792-831.
- [15] T. A. Revilla and V. Krivan, *Prey-predator dynamics with adaptive protection mutualism*, Appl. Math. Comput. **433**(2022): 127368.
- [16] M. Sen and M. Banerjee, A. Morozov, *Bifurcation analysis of a ratio-dependent prey-predator model with the Allee effect*, Ecol. Complex. **11**(2012), 12-27.
- [17] A. Singh and P. Deolia, *Bifurcation and chaos in a discrete predator-prey model with holling type-III functional response and harvesting effect*, J. Biol. Syst. **29**(2021), 1-8.
- [18] X. Y. Song and Y. F. Li, *Dynamic behaviors of the periodic predator-prey model with modified Leslie-Gower Holling-type II schemes and impulsive effect*, Nonlinear Anal. RWA **9**(2008), 64-79.
- [19] Z. J. Wen, *Study on Pattern Dynamics of Plankton and Fish System*, NCEPU J. Nat. Sci. Beijing, 2021.
- [20] Y. L. Zhu and K. Wang, *Existence and global attractivity of positive periodic solutions for a predator-prey model with modified Leslie-Gower Holling-type II schemes*, J. Math. Anal. Appl. **384**(2011), 400-408.

YANLIN MIN, CORRESPONDING AUTHOR, DEPARTMENT OF MATHEMATICS, NORTHWEST NORMAL UNIVERSITY, LANZHOU, 730070, P.R. CHINA

*Email address:* minyanlin2022@163.com

XIAOLING HAN, DEPARTMENT OF MATHEMATICS, NORTHWEST NORMAL UNIVERSITY, LANZHOU, 730070, P.R. CHINA

*Email address:* hanxiaoling9@163.com

CEYU LEI, DEPARTMENT OF MATHEMATICS, NORTHWEST NORMAL UNIVERSITY, LANZHOU, 730070, P.R. CHINA

*Email address:* leiceyu@126.com